

Review of fully coherent free-electron lasers

Chao Feng¹ · Hai-Xiao Deng¹

Received: 15 July 2018 / Revised: 23 August 2018 / Accepted: 24 August 2018 / Published online: 27 September 2018
© Shanghai Institute of Applied Physics, Chinese Academy of Sciences, Chinese Nuclear Society, Science Press China and Springer Nature Singapore Pte Ltd. 2018

Abstract Generation of intense, fully coherent radiation with wide spectral coverage has been a long-standing challenge for laser technologies. Several techniques have been developed in recent years to extend the spectral coverage in optical physics, but none of them hold the potential to produce X-ray laser pulses with very high-peak power. Urgent demands for intense X-ray light sources have prompted the development of free-electron lasers (FELs), which have been proved to be very useful tools in many scientific areas. In this paper, we give an overview of the basic principle of FELs, techniques for realizing fully coherent FELs, and the development of fully coherent FEL facilities in China.

Keywords Free-electron laser · Fully coherent · Seeded FEL · FEL oscillator

1 Introduction

Radiation from highly relativistic electron beams, such as those in synchrotron radiation facilities, has served as an important tool for probing a wide range of phenomena in

physics, chemistry, and biology. Recently, another revolutionary advance in light sources has been realized with the advent of the free-electron laser (FEL). Using coherent radiation from microbunched electron beams in a periodic magnetic field such as that of an undulator, a FEL is able to generate radiation with a brightness ten orders of magnitude higher than that of synchrotron radiation. Development of this next-generation light source is expected to satisfy the rapidly growing demand for photon sources within material and biology science.

One of the most exciting and impressive milestones in FEL development was operation of the first hard X-ray FEL facility, the Linac Coherent Light Source (LCLS), in 2009 [1]. More than 30 years of continuous advances in particle accelerators since the first operation of an infrared (IR) FEL made it possible to produce the first X-ray FEL pulse from the LCLS. The LCLS has been operating as a user facility for nearly 10 years, and tremendous breakthroughs in various fundamental research areas have been achieved. Motivated by the great success of the LCLS, several X-ray FEL facilities are currently under operation or under construction worldwide. Figure 1 shows the years of first lasing and typical operation wavelengths of existing FEL facilities worldwide. In Japan, the X-ray FEL facility SACLA achieved an unprecedented short wavelength of 0.06 nm in 2011 [2]. In South Korea, the PAL-XFEL delivered a 0.1 nm X-ray pulse with less than 20 fs timing jitter to users in 2017 [3]. Swiss FEL is now under commissioning and is scheduled for user operation in 2019 [4].

In addition, several superconducting radio frequency (RF) linac-based high-repetition-rate X-ray FELs are expected to generate radiation with even higher average brightness. European XFEL achieved first lasing and started operation in 2017 [5]. Construction of LCLS-II is now

This work was supported by the National Key Research and Development Program of China (No. 2016YFA0401900), the National Natural Science Foundation of China (Nos. 11475250 and 11775293), the Young Elite Scientist Sponsorship Program of CAST (2015QNRC001), and the Ten Thousand Talent Program.

✉ Hai-Xiao Deng
denghaixiao@sinap.ac.cn

¹ Shanghai Institute of Applied Physics, Chinese Academy of Sciences, Shanghai 201800, China

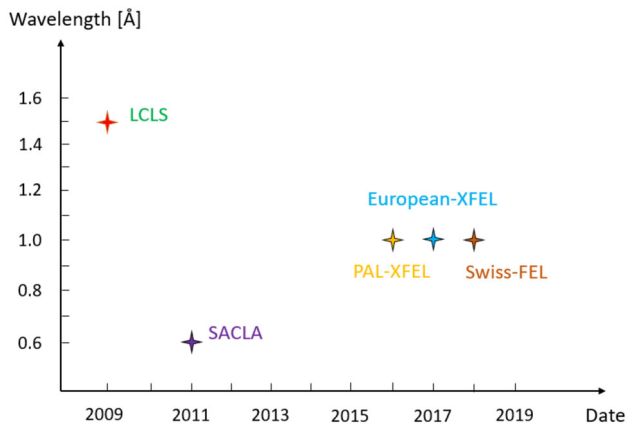


Fig. 1 (Color online) Years of first lasing and typical operation wavelengths of FELs worldwide

under way, and it will be opened to users in 2020 [6]. Further, construction of the first hard X-ray FEL facility in China, the Shanghai High-Repetition-Rate XFEL and Extreme Light Facility (SHINE), began in April 2018 [7].

Various operation modes have been developed for FELs as a next-generation light source to meet the requirements for a wide range of applications. The generation of intense ultrashort FEL pulses offers an opportunity for studying electric dynamics on the atomic or molecular scale and inspires new breakthroughs in ultrafast science. The pulse duration of self-amplified spontaneous emission (SASE) FELs is essentially determined by the length of the electron bunch, which is typically tens of femtoseconds. A short pulse can traverse samples and generate detectable signals faster than radiation-induced atomic motions, which is especially useful in biological studies. To further shorten the FEL pulse duration to the several attosecond levels, various ideas have been proposed for selecting a slice of the electron beam for lasing using an extremely short optical laser pulse modulation, a slotted foil, or a bunch tilt with subsequent orbit control [8–11]. Other schemes obtain short X-ray pulses by using a low-charge electron bunch [12] or compressing a normal electron beam nonlinearly [13].

In conventional X-ray FELs, a relative bandwidth of nearly 10^{-3} is routinely achieved, and even narrower bandwidths are pursued. However, the potential applications of broad-bandwidth operation have been recognized in recent years. XFEL pulses with a broad bandwidth of nearly 10^{-2} are useful for X-ray crystallography and many spectroscopy experiments. Further, it is convenient for broad-bandwidth FEL to tune the radiation wavelength in a broad range by simply using a monochromator. Two methods are used to generate broad-bandwidth FELs. One is to use electron beams with a large energy chirp so that electrons with different energies lase at different

wavelengths. High-energy chirped electron beams can be obtained effectively by overcompressing the electron beam in the last bunch compressor [14, 15]. In addition, an energy chirp can be induced by the strong space charge effect in an extremely compressed electron beam [16]. Another method is to let different parts of an electron beam experience different undulator fields. This can be achieved by sending appropriate head–tail tilted electron bunches into a transverse gradient undulator (TGU) [17] or a planar undulator with a natural gradient [18].

High-intensity FEL pulses are a promising tool for revolutionary applications in X-ray diffraction before destruction [19] and nonlinear X-ray science [20]. A new chapter in the history of high-intensity X-ray–matter interaction opened with the 10^{17} – 10^{21} W/cm² X-ray pulse delivered by the LCLS. A high-gain FEL amplifier, which typically works in the linear exponential gain regime, is the first option for generating high-peak-power radiation at various wavelengths. However, saturation occurs when electrons lose a significant amount of energy and start dephasing in the ponderomotive potential bucket. The FEL efficiency is given by the Pierce parameter, which is typically limited to 0.1%. A solution to this problem is to maintain the FEL resonance by carefully matching the undulator parameters with the electron bunch energy after saturation [21]. Theoretical studies have shown that the undulator tapering technique is able to dramatically increase the FEL peak power to the terawatt level as well as increase the energy extraction efficiency by more than two orders of magnitude [22–24]. A recent experiment demonstrated that an energy extraction efficiency as high as 30% can be obtained by using a 200 GW, 10.3 μ m CO₂ laser seed and a strongly tapered undulator [25]. Much effort has been made to increase the efficiency of FELs in the short-wavelength regime, and various advanced methods such as machine learning and genetic algorithm are used for undulator tapering optimization.

Owing to the relatively high beam energy required, the typical X-ray FEL facility is up to several miles long. Methods of reducing the cost and size of an X-ray FEL are always an intriguing topic. On one hand, it might be possible to obtain a compact light source by enhancing the accelerator gradient and therefore shortening the accelerator. The use of advanced accelerator concepts such as the laser plasma accelerator [26], which is able to achieve a 10–100 GeV/m gradient, is now under investigation. On the other hand, some efforts have been made to significantly reduce the required electron beam energy by using Compton scattering [27] or various harmonic lasing techniques.

Well-defined polarization is highly desirable in studies of ultrafast magnetic phenomena and material science

[28, 29]. To obtain FEL radiation with variable polarization, crossed-planar undulators [30–32] and elliptical permanent undulators [33, 34] are two options. The crossed-planar undulator consists mainly of horizontal and vertical undulators and a phase shifter. It enables flexible polarization switching at a high rate, but it suffers from a relatively low degree of polarization because the two linearly polarized lasers are emitted separately at two undulators. Recently, owing to its ability to produce reliable highly polarized FEL pulses, the elliptical undulator has been implemented in several facilities. Radiation from the Delta undulator at the LCLS has exhibited an extremely high degree of circular polarization compared with that of crossed-planar undulators [31, 32]. However, changing the polarization at kilohertz rates by mechanically adjusting the Delta undulator is challenging.

Further, another important topic is the generation of fully coherent X-ray pulses, which will support many applications, including soft X-ray resonant inelastic scattering, spectroscopic studies of correlated electron materials, and holographic, diffractive, or lensless imaging. In this review, we focus on the fully coherent FEL. An overview of the basic principles of FELs, techniques for realizing fully coherent FELs, and the development of fully coherent FEL facilities in China is given.

2 From low-gain to high-gain FELs

The FEL was invented by Madey [35]. He pointed out that a finite gain is available in stimulated emission when a relativistic electron beam passes through a periodic magnetic field. Further, a FEL at wavelength λ can be generated under the resonant condition between the electron beam energy γ , radiation wavelength λ , undulator period λu , and scaled magnetic field intensity K :

$$\lambda = \frac{\lambda u}{2\gamma^2} \left(1 + \frac{K^2}{2} \right), \tag{1}$$

which guarantees continuous energy extraction from an electron bunch to radiation. One advantage of FELs over traditional lasers is the ability to obtain a flexible wavelength range extending from the terahertz to X-ray regions by simply adjusting the electron beam energy or undulator parameters. Madey’s calculation illustrated the possibility of using amplifiers and oscillators as tunable coherent radiation sources in the ultraviolet (UV) and X-ray regions. After the FEL concept was proposed, the low-gain FEL was quickly demonstrated by operation of a FEL oscillator (FELO) above the threshold at a wavelength of 3.4 μm at Stanford University [36].

Using free electrons as gain media, many low-gain FELOs in the long-wavelength regime, e.g., terahertz, IR,

and UV, have been constructed as user facilities at universities worldwide. One of the most productive FELOs is FELIX at Radboud University [37], which produces versatile fully coherent radiation in the IR and far-infrared (FIR) regions for users. As shown in Fig. 2, 10 Hz electron macropulses from the thermal cathode gun are accelerated by two linacs to 15–25 and 25–45 MeV. The electron beams are then bent into two FELOs and lase at 16–250 μm and 5–30 μm , respectively. The output average power of the macropulses is nearly 10 W, and the output peak power of the micropulses is at the megawatt level. FELIX has proved to be useful for studies of solid-state dynamics, atomic clusters, and magnetic materials.

Despite the great success of FELOs at long wavelengths, it is challenging to build an X-ray FELO (XFEL) owing to a lack of high-reflectivity mirrors at short wavelengths. To circumvent the requirement for an optical cavity, SASE [38, 39] was proposed, which takes advantage of a single-pass high-gain FEL. As shown in Fig. 3, a SASE FEL contains a long undulator section. It starts with electron beam spontaneous radiation and gradually develops electron beam microbunching at the radiation wavelength. The positive feedback between the electron beam microbunching and coherent radiation leads to exponential growth of the radiation power. As the electron beam energy spread grows significantly, the SASE FEL reaches saturation, with typically a gigawatt-level output peak power. The radiation wavelength of a SASE is theoretically unbounded.

The behavior of a one-dimensional high-gain FEL using a cold electron beam can be characterized well by the so-called Pierce parameter [39]:

$$\rho \equiv \frac{1}{2\gamma} \left[\frac{I}{IA} \frac{\lambda u^2 K^2 [JJ]^2}{8\pi^2 \epsilon \beta} \right]^{1/3}, \tag{2}$$

where I is the peak current, IA is the Alfvén current, ϵ is the electron beam emittance, β is the beta function, and the factor $[JJ]$ arises from electron longitudinal oscillation, which modifies the average coupling between electrons and the radiation field. The FEL power growth is characterized by the gain length,

$$L_g \approx \frac{\lambda u}{4\pi\sqrt{3}\rho}, \tag{3}$$

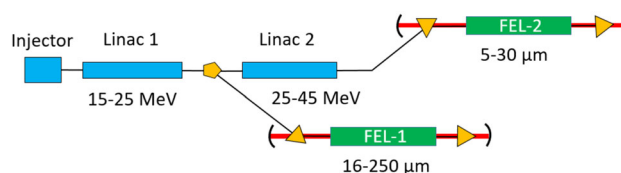


Fig. 2 (Color online) Layout of FELIX facility at Radboud University

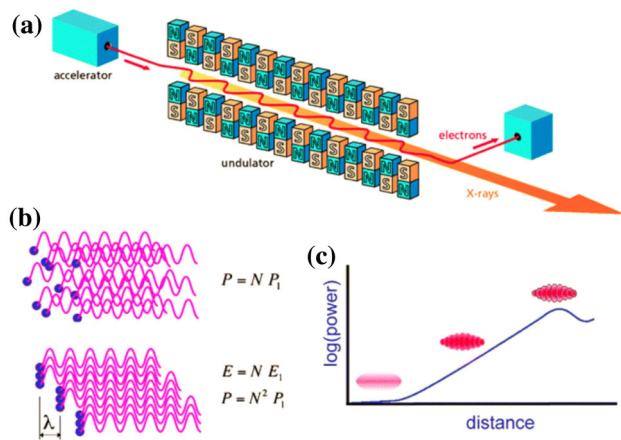


Fig. 3 (Color online) Principle of SASE [40]. **a** Schematic of SASE FEL that contains a long undulator. **b** Coherent radiation induced by electron beam microbunching developed along the undulator. **c** Exponential growth of radiation power along the undulator

which means that the undulator length required for a given radiation power grows by a factor of e .

The gain length determines the total undulator length required for saturation, which is important in FEL design. Formula (3) evaluates the gain length of a FEL with an ideal cold electron beam. To limit the gain length to a reasonable value, the impact of the beam parameters, including the energy spread and emittance, should be considered. A large energy spread degrades the electron microbunching owing to the presence of various longitudinal velocities. In a SASE FEL, electrons with different energies would be resonant with different radiation frequencies; thus, to pursue highly efficient energy conversion, the electron beam energy spread should be less than the FEL gain bandwidth, which equals the Pierce parameter, i.e.,

$$\frac{\delta\gamma}{\gamma} \leq \rho. \quad (4)$$

The requirement for the electron beam emittance is similar to that for the energy spread. As an electron oscillates around the central axis in an undulator, the transverse momentum changes, and so does the longitudinal momentum. Hence, the limit on the electron beam emittance is [41]

$$\varepsilon \leq \frac{\beta\lambda}{\lambda u} \rho. \quad (5)$$

The development of accelerator techniques, especially the generation of high-brightness electron beams (with a small energy spread and low emittance) from a photocathode RF gun, is critical for the realization of X-ray SASE FELs. Some proof-of-principle experiments on SASE were conducted at a wavelength of 16 μm at University of

California, Los Angeles (UCLA) [42]. Scientists in Hamburg then recognized the opportunity to build an extreme ultraviolet (EUV) FEL facility known as Free-Electron LASer in Hamburg (FLASH) [43]. This achievement of pioneering high-gain FEL facilities stimulated the construction of soft X-ray FELs and the LCLS [1].

The last 10 years have witnessed the development of potential applications of X-ray FELs in various research areas: atomic, molecular, and optical physics; condensed matter physics; matter in extreme conditions; chemistry and soft matter, and biology [44]. Several X-ray FEL facilities have been constructed and opened for user operation worldwide in recent years, as shown in Table 1. Most of these facilities are based on the SASE principle. Starting from the electron beam density shot noise, SASE is able to generate X-rays with nearly perfect transverse coherence; however, its further applications are limited by the intrinsic poor longitudinal coherence. Therefore, methods for producing fully coherent X-ray FELs have attracted tremendous attention after the first light of LCLS.

3 Fully coherent FELs

To improve the temporal coherence of SASE and achieve fully coherent FELs, various SASE-based, external seeding- or oscillator-based techniques have been proposed and partially experimentally demonstrated in recent years.

3.1 Beyond SASE

The temporal coherence of SASE can be significantly improved by using the self-seeding scheme [45, 46], which employs a double undulator configuration, as shown in Fig. 4. The self-seeding technique uses a monochromator together with a bypass chicane to obtain monochromatic light from SASE itself and then amplify it to saturation. The undulator is divided into two parts by the monochromator. The first undulator section is used to generate a normal SASE radiation pulse that is interrupted well before saturation. Then, the monochromator is employed to purify the spectrum and provide a coherent seeding signal at a short wavelength, while the bypass chicane is used to delay the electron beam and wash out the microbunching formed in the first undulator section. Next, the seeding signal and the electron beam are simultaneously sent into the second undulator section to interact with each other and produce an intense coherent X-ray pulse.

Self-seeding FELs can be categorized as using soft or hard X-ray self-seeding depending on the monochromator materials chosen for different photon energy ranges. Generally, grating-based monochromators can be applied for the photon energy range of 0.4–1.5 keV, whereas crystal-

Table 1 X-ray FEL facilities worldwide

Facility	FEL operation modes	Electron beam energy (GeV)	Photon energy coverage (keV)
LCLS	SASE, self-seeding	14.3	1–15
LCLS-II	SASE, self-seeding	4	0.2–5
FLASH	SASE	1.25	0.014–0.3
European XFEL	SASE, self-seeding	17.5	8.4–30
SACLA	SASE, self-seeding	8	0.44–20
FERMI	external seeding	1.5	0.0124–0.3
PAL-XFEL	SASE, self-seeding	10	0.124–12.4
Swiss FEL	SASE	5.8	0.177–12.4
SXFEL	SASE, external seeding	1.5	0.1–0.6
SHINE	SASE, self-seeding, external seeding	8	0.425

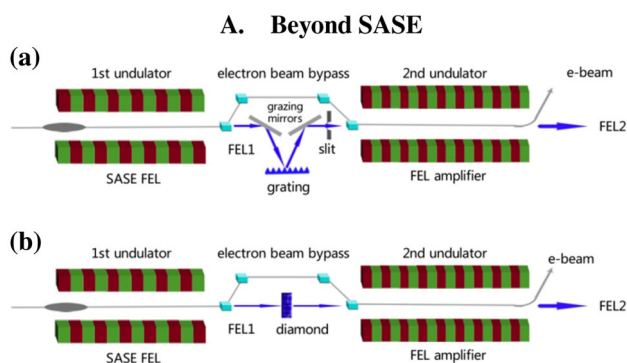


Fig. 4 (Color online) Schematic layouts of soft X-ray self-seeding (a) and hard X-ray self-seeding (b) [47]

based monochromators are suitable for the photon energy range of 3–12 keV. Both soft X-ray and hard X-ray self-seeding have been demonstrated at the LCLS in recent years [48, 49]. The main experimental results are shown in Fig. 5, where one clearly finds that the spectral bandwidth

of SASE can be reduced by dozens of times by self-seeding techniques in both the soft and hard X-ray regions. To date, self-seeding is one of the most reliable techniques to provide high-peak-power, ultrashort X-ray light pulses with extraordinary coherence both transversely and longitudinally. However, the large shot-to-shot power fluctuation of self-seeding schemes has limited their application. Further, a photon energy gap still exists between 1.5 and 3 keV that cannot be fully covered by present self-seeding schemes owing to a lack of suitable materials for the monochromator. In addition, recent spectral measurements at the LCLS showed that there is a pedestal-like sideband [48] in the spectrum of soft X-ray self-seeding owing to microbunching instability effects in the linac, which degrades the FEL longitudinal coherence and thus limits the user applications. In order to overcome these problems and further improve the quality of the radiation pulse, several methods have been proposed recently [50–52]. Currently, in order to mitigate the effects of thermal loading on the monochromator when the X-ray repetition

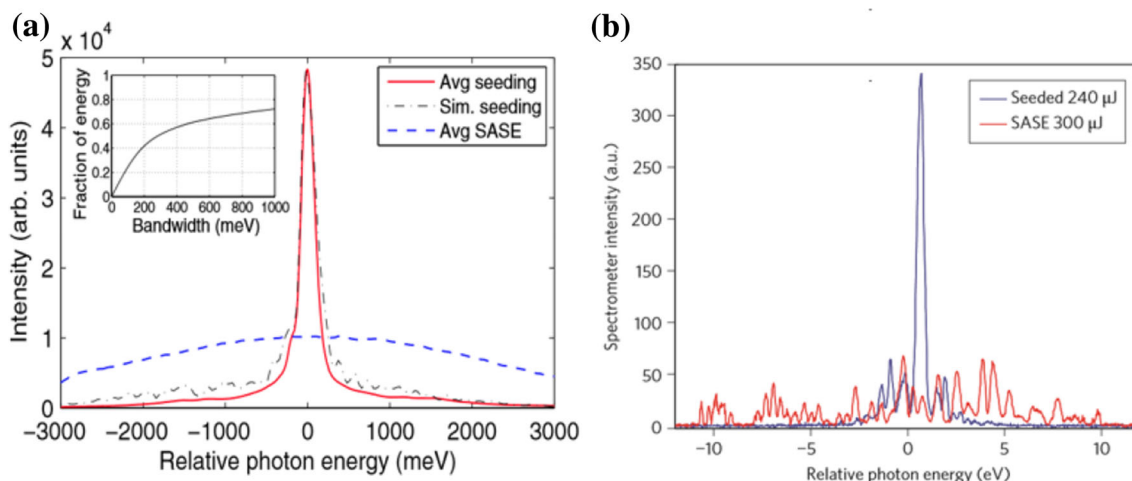


Fig. 5 (Color online) Experimental results of soft X-ray (a) and hard X-ray (b) self-seeding [48, 49]

rate is high, multistage self-seeding has been proposed and is under investigation.

The longitudinal properties of the SASE FEL are determined mainly by the slippage length or cooperation length of the radiation. An alternative way to improve the longitudinal coherence of SASE is to enhance the FEL slippage, which provides an in situ method for communicating phase information over larger portions of the electron beam. Several techniques based on this principle, such as high-brightness SASE [53], improved SASE [54], purified SASE [55], and harmonic lasing self-seeding (HLSS) [56], have been developed. Recent results of HLSS at FLASH have demonstrated that the spectral bandwidth of SASE can be reduced by several times [57]; this result is not as good as that obtained by self-seeding but can still significantly increase the spectral brightness. Unlike that of self-seeding, the central wavelength of slippage-boosted SASE is still determined by the electron beam energy, which results in fluctuation of the central wavelength from shot to shot. However, the advantage of slippage-boosted SASE is that the output pulse energy is insensitive to the beam energy fluctuation.

3.2 Seeded FELs

The temporal coherence and intrinsic pulse energy fluctuations of the SASE and self-seeding schemes can be further improved by using seeded FELs with external seed lasers. The output properties of a seeded FEL directly reflect the seed laser's attributes, which ensures a high degree of temporal coherence and small pulse energy fluctuations with respect to SASE. Compared to self-seeding, seeding with external lasers has an additional advantage in that the FEL pulse is locked to an external signal. This allows more precise temporal synchronization, which is especially important for pump-probe experiments. The schematic layouts of the main types of seeded FELs are given in Fig. 6.

The straightforward seeded FEL, which is called a directly seeded FEL, is illustrated in Fig. 6a. An intense laser source is injected directly into the undulator to suppress the incoherent spontaneous emission at the very beginning of the undulator and dominates the FEL gain process. At short wavelengths, the only available coherent source is generated through the high-harmonic generation (HHG) process, which is facilitated by the highly nonlinear interaction of a very intense optical laser pulse with a rare gas. The HHG direct seeding scheme has been successfully demonstrated at EUV wavelengths [58–60]. However, owing to the rapid intensity drop of HHG at very high harmonics, HHG direct seeding is still not suitable for X-ray FEL generation.

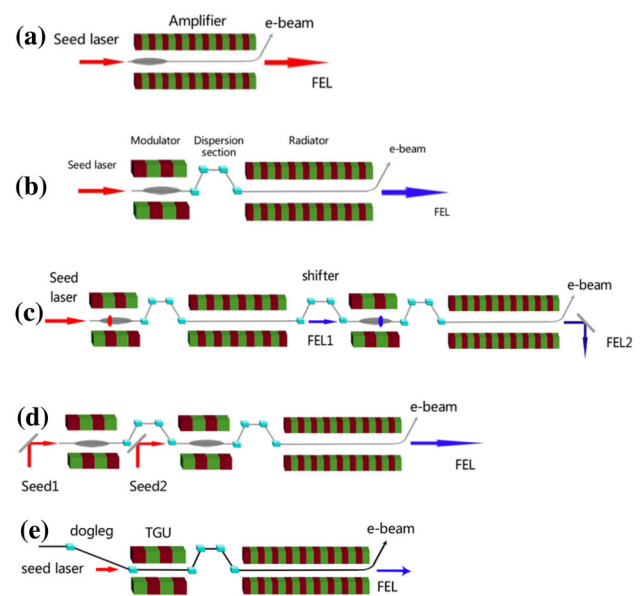


Fig. 6 (Color online) Schematic layouts for various seeding techniques. **a** Directly seeded FEL, **b** HGHG, **c** multistage HGHG, **d** EEHG, **e** PEHG [47]

To circumvent the need for a seed source at short wavelengths, frequency up-conversion schemes that rely on optical-scale electron beam phase space manipulation have been envisioned to convert commercially available seed sources to shorter wavelengths. The first frequency up-conversion scheme is called high-gain harmonic generation (HGHG) (Fig. 6b) [61] and uses two undulators and a dispersion section. A seed laser pulse is first used to interact with the electrons in a short undulator, called the modulator, to generate a sinusoidal energy modulation in the electron beam longitudinal phase space at the scale of the seed laser wavelength. The formed energy modulation is then developed into an associated density modulation by a dispersive magnetic chicane called the dispersion section. The high-harmonic components of the seed laser frequency can be generated in the electron beam density distribution, making this approach feasible for reaching shorter wavelengths [62]. However, significant bunching at higher harmonics is usually needed to strengthen the energy modulation in HGHG, which will result in degradation of the amplification process in the radiator. Thus, the requirement of FEL amplification on the beam energy spread makes it impossible to reach short wavelengths in single-stage HGHG. For this reason, the multistage HGHG scheme (Fig. 6c) [63, 64] has been proposed. A FEL generated by an intermediate radiator can be used as the seed laser for the following HGHG stage, with the help of the “fresh bunch” technique. Analysis within the framework of idealized models suggests that two-stage HGHG can produce fully coherent soft X-rays. The two-stage

HGHG scheme has been adopted by FERMI [65] and the Shanghai Soft X-ray FEL Facility (SXFEL) [66] as the baseline for FEL operation.

In order to improve the frequency multiplication efficiency of a single stage, more complicated phase space manipulation techniques have been developed. One of them, echo-enabled harmonic generation (EEHG) (Fig. 6d) [67, 68], employs two modulators and two dispersion sections to introduce an echo effect into the electron beam phase space to enhance the frequency multiplication efficiency with a relatively small energy modulation. Analytical calculations and experimental results imply that single-stage EEHG is able to generate high-power soft X-ray radiation with a narrow bandwidth close to the Fourier transform limit directly from a UV seed source [69–73]. Although the EEHG scheme has a remarkable up-frequency conversion efficiency, it is still very difficult to use single-stage EEHG to generate hard X-ray radiation directly from a commercially available UV seed laser. One possible way to further increase the harmonic up-conversion number to achieve subnanometer wavelengths is to combine the EEHG with the “fresh bunch” technique [74–76].

Although EEHG has an unprecedented up-frequency conversion efficiency and enables the generation of ultra-high harmonics with a relatively small energy modulation, its configuration is more complex than that for HGHG, and the coherent synchrotron radiation and incoherent synchrotron radiation effects induced by the large chicane may smear out the fine structure in longitudinal phase space. Recently, the idea of using a TGU to mitigate the effects of electron beam energy spread has been proposed as the phase-merging enhanced harmonic generation (PEHG) technique [77, 78]. A schematic layout of PEHG is shown in Fig. 6e. Although the TGU is originally used to compensate for the effects of beam energy spread by making every electron satisfy the resonant condition, this novel scheme utilizes a different operating regime of the TGU. When the transversely dispersed electrons pass through the TGU modulator, around the zero-crossing of the seed laser, electrons with the same energy will merge into the same longitudinal phase, which makes it possible to generate fully coherent short-wavelength radiation at very high harmonics of the seed. Further studies have shown that the function of the TGU can also be performed by a tilted seed laser [79] or magnetic dipole [80] or by using the natural transverse gradient of a normal undulator [81, 82]. A proof-of-principle PEHG experiment is planned at the SXFEL [83].

3.3 X-ray FEL oscillators

An alternative way of generating fully coherent stable X-ray FEL pulses is by an XFELO. The XFELO concept, which employs crystals as cavity mirrors, was proposed at the same time as SASE. However, the XFELO did not receive much attention owing to the shortage of perfect crystal mirrors that are able to provide sufficient feedback. In 2009, the first demonstration of high-reflectivity Bragg diffraction at normal incidence of a diamond crystal paved the way to realization of an XFELO [84]. The XFELO concept was resurrected, and a configuration based on the energy recovery linac was proposed [85]. In addition, the generation of a high-brightness, high-repetition-rate (1 MHz) electron beam from an advanced superconducting linear accelerator offers another potential option for high-current XFELO operation. With the ability to produce fully coherent X-ray pulses of 10^9 – 10^{11} photons at a repetition rate of 1–100 MHz, the XFELO attracted much attention.

A schematic view of the XFELO is shown in Fig. 7. A high-repetition-rate relativistic electron beam from a superconducting linac is injected into the XFELO. An undulator with an appropriate length is installed inside the X-ray cavity. The X-ray pulse starts from spontaneous radiation from the leading electron bunch inside the undulator, and the power grows exponentially if the single-pass FEL gain exceeds the cavity round-trip loss. XFELs work in the low-gain regime with a single-pass gain of typically less than 10, and they require hundreds of round trips before power saturation. The X-rays are coupled out through crystal mirror transmission. Transverse X-ray mode is controlled by external focusing elements such as multilayer curved mirrors or compound refractive lenses, whereas the longitudinal coherence is improved significantly by narrow-bandwidth Bragg diffraction [87]. A zigzag optical cavity configuration is used to improve the wavelength tunability [88].

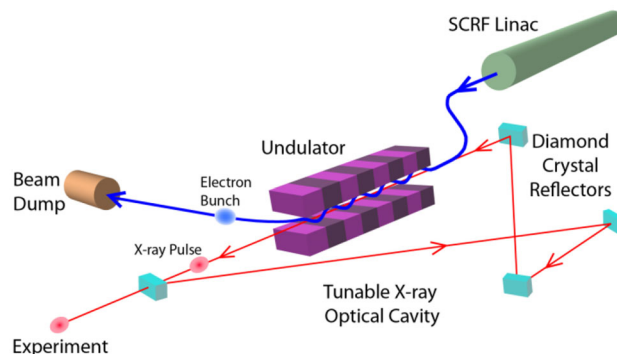


Fig. 7 (Color online) Schematic view of XFELO [86]

XFEL physics, which includes the X-ray optics, FEL gain, and Bragg diffraction, is more complicated than that of a single-pass high-gain FEL. Thus, numerical simulation is typically used for its theoretical study. Recently, a three-dimensional Bragg diffraction code called BRIGHT, which can be used with GENESIS and Optical Propagation Code (OPC), was developed for fully three-dimensional XFEL simulation [89]. The three-dimensional Bragg diffraction formula is obtained using dynamic diffraction theory with some reasonable approximations. In addition, a simplified one-dimensional theoretical XFEL model is established for fast optimization in XFEL design. It exploits FEL low-gain theory in the saturation regime to calculate the single-pass gain at different radiation powers and then obtains the X-ray pulse power evolution through iteration [90].

Because XFELs work in the low-gain regime, a reliable X-ray output pulse energy is ensured. The maximum energy conversion efficiency of a FEL with a constant undulator parameter is inversely proportional to the number of undulator periods. New schemes for further improving the efficiency of XFELs have been proposed continuously in recent years. The gain cascading scheme, which controls the delay elements between the stages of the undulators to allow electron beam lasing at various locations inside different undulators, is capable of increasing the energy extraction efficiency and output peak power owing to the shortening of the undulator length at each stage [91]. As shown in Fig. 8, one numerical example of a four-stage gain cascading scheme predicts that the peak radiation power can be increased by a factor of 8.6, while the energy extraction efficiency is enhanced by a factor of 2.5 [91]. Another scheme uses the XFEL output as a fully coherent stable seed for a subsequent tapered FEL amplifier, like the master oscillator and power amplifier (MOPA)

configuration used by the laser community. The challenge of MOPA is that the enhanced energy spread inside the XFEL would degrade the efficiency of the subsequent amplifier. A simple solution would be to employ a chirped electron beam and make the bunch tail provide a FEL gain inside the oscillator with bunch head lasing at the FEL amplifier. A start-to-end simulation illustrates that this configuration is capable of generating fully coherent stable X-rays with a peak power at the terawatt level [92].

Another method of improving XFEL performance is the generation of higher X-ray photon energies by harmonic lasing [93]. The key to achieving harmonic lasing inside an XFEL is to make the radiation power buildup more favorable at the harmonic wavelength than at the fundamental one. This is realized by using a combination of a phase shifter, which disturbs the FEL gain of the fundamental wavelength, and a crystal cavity mirror, the Bragg energy of which is chosen to be the harmonic photon energy. Furthermore, stabilization of the XFEL cavity by using the narrow nuclear resonance lines of nuclei such as ^{57}Fe as a reference has been investigated [94]. The temporal coherent length of the XFEL output can be further increased dramatically, from picoseconds to microseconds or even longer. This indicates excellent potential for use of XFELs as time and length standards, and it is expected to contribute to the development of X-ray quantum optics.

Recently, a gain-guided XFEL was proposed, which avoids the need for the X-ray focusing elements used in the conventional XFEL configuration [95]. The FEL gain of the electron beam is used to focus the X-rays transversely and keeps them in a stable mode. Theoretical analysis and three-dimensional simulations have shown that the gain-guided XFEL is capable of generating fully coherent X-rays with an energy conversion efficiency comparable to that of a normal XFEL. In an initial exploration of a

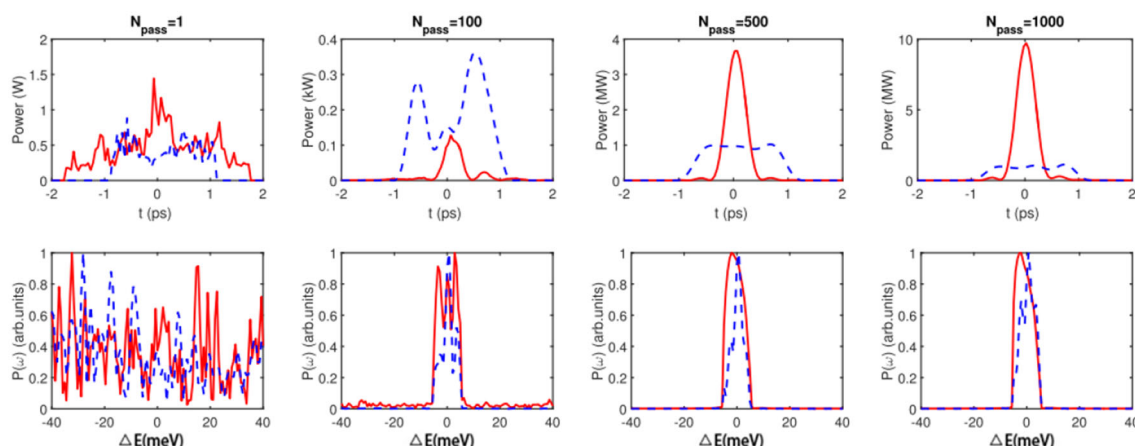


Fig. 8 (Color online) Temporal and spectral profile of the output 0.1 nm pulse in the normal FEL (blue dashed line) and four-stage undulator cascaded FEL (red solid line) [91]

novel and simple XFEL configuration, a gain-guided XFEL relaxed the heat loading as well as the angular misalignment requirement of the crystal mirrors, and it might dominate future XFEL designs.

Intensive theoretical studies recently proved that XFELs are feasible and are capable of producing fully coherent hard X-ray pulses with unprecedented stability. Although there might be some technical problems, including crystal heat loading, cavity mirror angular stability, and resilience to radiation damage, scientists worldwide are designing XFELs for their own XFEL facilities based on superconducting linacs. Vigorous and fruitful investigation of the interaction between X-rays and crystal mirrors is expected to greatly promote the construction of XFELs [96]. The spectral brightness of the XFEL output is more than two orders of magnitude higher than that of SASE. This extraordinary X-ray source is complementary to SASE mode and is expected to contribute significantly to scientific experiments such as X-ray inelastic scattering spectroscopy and nuclear resonant scattering, bulk-sensitive Fermi surface studies, X-ray imaging with near-atomic resolution, and X-ray photon correlation spectroscopy.

4 FEL facilities in China

FEL development in China started in the 1980s. During the 1980s and 1990s, the Shanghai Institute of Optics and Fine Mechanics, University of Science and Technology of China (USTC), Institute of High Energy Physics (IHEP), Chinese Academy of Engineering Physics (CAEP), China Institute of Atomic Energy, Southwest Institute of Applied Electronics, University of Electronic Science and Technology of China, and Shanghai Institute of Applied Physics (SINAP) worked on FEL-related projects covering the spectral regions from millimeter to FIR and IR to UV. The high-gain FEL program in China began in 1998, when the Shanghai Deep Ultraviolet (SDUV) project was proposed as a collaboration between SINAP, IHEP, and USTC. Later, the Accelerator Lab of Tsinghua University in Beijing joined the project. In this section, we review the development of FEL facilities in China.

4.1 Low-gain FELs in China

The Beijing FEL (BFEL) at IHEP is an IR FEL. It successfully lased at 10.6 μm in May 1993 [97], making it the first FEL to lase in Asia. The BFEL became a user facility after saturation was achieved in 1994. The induction-linac-based FEL amplifier at the China Academy of Engineering Physics (CAEP) achieved first lasing at 34 GHz with a peak power of 10 MW in April 1993. First

lasing of the CAEP FIR FEL at a central wavelength of 115 μm was observed in March 2005 [98, 99], marking the birth of coherent terahertz sources in China.

The CAEP, together with Peking University and Tsinghua University, developed a terahertz FEL (CTFEL) facility, which is the first high-average-power FEL user facility in China [100]. CTFEL consists mainly of a GaAs photocathode high-voltage DC gun, a 1.3 GHz 2×4 -cell superconducting RF linac, a planar undulator, and a quasi-concentric optical resonator. First lasing of CTFEL was realized in 2017 [101]. Since then, stable terahertz pulses from CTFEL have been delivered to user experiments. The repetition rate of the terahertz beams is 54.17 MHz, and the terahertz frequency can be adjusted continuously from 1.87 to 3.8 THz. The average output power of the macropulse is more than 10 W, and the peak power exceeds 0.5 MW [102]. A fast machine protection system and continuous-wave (CW) operation are currently under development and will be realized soon. Moreover, CTFEL is expected to be upgraded to cover the terahertz band from 1 to 10 THz and greatly promote the development of terahertz science as well as many other cutting-edge fields in the future.

In 2014, construction of Tunable Infrared Laser for Fundamental of Energy Chemistry (FELiChEM), a new IR FEL dedicated to fundamental energy chemistry research, began at USTC. The IR FEL is composed of two FELs that cover the spectral ranges of 2.5–50 μm and 40–200 μm , respectively, and are driven by one electron linac. Two 2 m accelerating tubes are used to accelerate the electron beam, and the maximum electron energy is 60 MeV [103, 104]. The installation of the FEL machine is complete, and commissioning will start soon. According to the design, FELiChEM will be a state-of-the-art IR FEL with an intense pulse energy of 50 μJ for micropulses and 100 mJ for macropulses, a micropulse length of 1–5 ps, a spectral bandwidth of 13%–0.2%, and continuous wavelength tunability [103, 105].

4.2 SDUV–FEL

The SDUV–FEL was jointly funded by the Chinese Academy of Sciences, Ministry of Science and Technology of China, and National Natural Science Foundation of China. It officially began as R&D of a 100 MeV linac, a photocathode RF gun, and radiator undulators toward an HGHG test facility in 2002 [106]. The SDUV–FEL is a multipurpose test facility for studies of the FEL principle and is capable of testing various novel high-gain FEL schemes by changing the layout of the machine. The design and relevant R&D projects at this facility have been under way since 2000. The construction of this machine with a single-stage HGHG setup began in 2009. Figure 9 shows the gain curve of 347 nm HGHG operation at the SDUV–

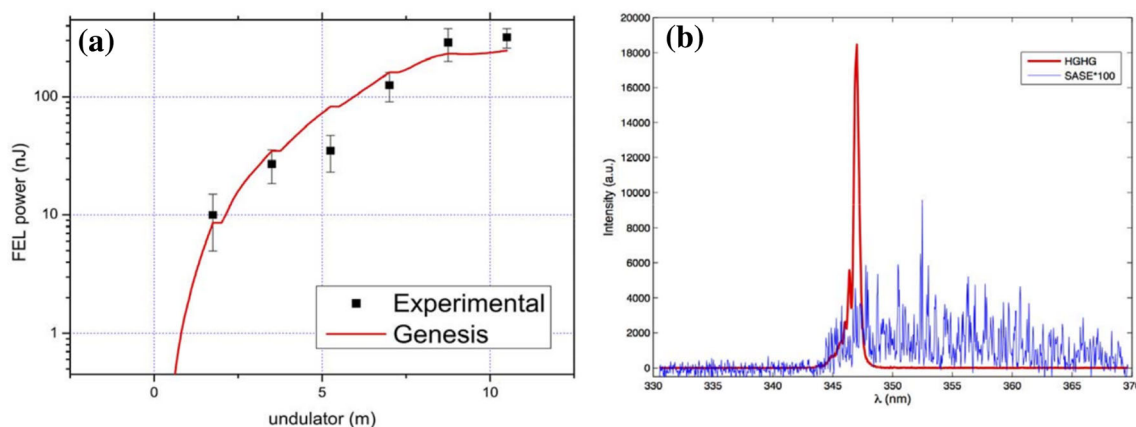


Fig. 9 (Color online) Gain curve of 347 nm HGHG operation (a), comparison of output spectra of HGHG and SASE at the SDUV-FEL (b) [107]

FEL (Fig. 9a), as well as the output spectrum of HGHG and SASE (Fig. 9b). An upgrade of this machine for a two-stage HGHG demonstration was finished in 2012.

After dramatic evolution during the past decade, the final layout of the SDUV-FEL can be divided into an accelerator component and a FEL component. The accelerator component consists of a 1.6-cell BNL-type photocathode RF gun operating at 2856 MHz (provided by Tsinghua University), five SLAC-type linac sections operating at the same frequency, a four-dipole chicane, and a number of quadrupole and corrector magnets for beam optics and orbit control. Downstream of the linac, there are undulator components for the FEL experiment. The undulator system is quite complex and includes three modulators, three dispersion sections, two radiators, one crossed undulator, and one fresh bunch chicane. With this undulator configuration, we are able to carry out a variety of FEL experiments [107], namely SASE, HGHG, and EEHG, as well as two-stage HGHG. Very soon after commissioning and performance optimization of the photoinjector and linac, a series of FEL experiments [31, 71, 108–110] was conducted at the SDUV-FEL beginning in September 2009. The following milestones have been achieved:

- December 2009: SASE experiment and exponential gain
- October 2010: HGHG saturation
- October 2010: Measurement of the slice energy spread of the energy beam
- April 2011: First lasing of an EEHG FEL
- August 2011: Demonstration of widely tunable HGHG
- April 2012: First signal from two-stage HGHG
- November 2013: Polarization control by a crossed undulator
- April 2014: FEL spectrum control by a corrugated structure

4.3 DCLS

High-brightness, ultrafast FEL pulses in the EUV wavelength region are an ideal light source for excitation of valence electrons and ionization of molecular systems with very high efficiency. They are quite helpful for studies of important dynamic processes in physical, chemical, and biological systems. The Dalian Coherent Light Source (DCLS) was launched by the Dalian Institute of Chemical Physics and SINAP, Chinese Academy Sciences, and funded by the National Natural Science Foundation of China. It is planned to deliver an optical beam of 50–150 nm in picoseconds or 100 fs for research. HGHG is the first choice for an EUV FEL with a narrow bandwidth and stable output power. After eight months of installation and machine commissioning, a 300 MeV electron beam was achieved with a peak current of more than 300 A, and the emittance was less than 1.5 mm mrad. The FEL pulse energy of an individual pulse at 133 nm nearly exceeded 200 μ J with a 266 nm seed laser in January 2017. Fine tuning of the undulator taper increased the FEL pulse energy by almost 100%. User experiments began in June 2017. The photodissociation dynamics of H_2O via the \tilde{F} state at 111.5 nm, which had been very difficult to study owing to the lack of a powerful and tunable EUV light source, was first investigated at the DCLS [111].

4.4 SXFEL

The SXFEL is the first Chinese coherent light source in the wavelength range of 20–2 nm [112, 113]. It is based on a 1.5 GeV normal conducting high-gradient C-band linac and currently contains two FEL beamlines, a seeded FEL beamline and a SASE beamline, and five experimental stations. This facility is being developed at the Shanghai Synchrotron Radiation Facility (SSRF) campus of SINAP

in two steps, the SXFEL test facility (SXFEL-TF) and the SXFEL user facility (SXFEL-UF). Currently, the 0.84 GeV linac-based SXFEL-TF is under commissioning, with the goal of testing the key-related technologies and two-stage seeded FEL. Further, the user experiment-oriented SXFEL-UF is being developed at designated wavelengths down to the water window region toward user service in 2019. The layouts of the SXFEL-TF and SXFEL-UF are compared in Fig. 10.

The SXFEL will be used to adopt novel seeded FEL schemes such as EEHG or EEHG cascading to further improve the ultrahigh harmonic up-conversion efficiency, and it will be capable of controlling the FEL output properties such as the central wavelength, pulse duration, polarization, synchronization, and longitudinal phase, and implementation of multicolor operation in the near future.

4.5 SHINE

SHINE is a newly proposed high-repetition-rate X-ray FEL facility based on an 8 GeV CW superconducting RF linac [7]. It will be located at Zhangjiang High-tech Park, which is close to the SSRF campus in Shanghai, at a depth of 30 m underground and with a total length of 3.2 km, as shown in Fig. 11. SHINE will have five shafts, one accelerator tunnel, and three parallel undulator tunnels with three following beamline tunnels, where each undulator tunnel will be able to accommodate two undulator lines. In its initial phase, SHINE consists of an 8 GeV CW superconducting RF linac, three undulator lines, three following FEL beamlines, and ten experimental end-stations. The end-stations are distributed in the near experimental hall in Shaft 4 and the far experimental hall in Shaft 5. The first three undulator lines will be located in two undulator tunnels. Using these three undulator lines, SHINE will be used to generate brilliant X-rays between 0.4 and 25 keV at pulse repetition rates of up to 1 MHz. Beyond SASE, SHINE will be able to deliver fully coherent FEL pulses at

different photon energies by using specified narrow-bandwidth schemes at different FEL lines.

5 Summary and outlook

The last several decades have witnessed stunningly rapid development of FELs ranging from well-established successful low-gain FELs at long wavelengths to high-gain FEL amplifiers at short wavelengths. This revolutionary light source has opened up vast research frontiers in physics, chemistry, and biology. The growing demand for photons with different attributes stimulated FEL development in various directions: generation of ultrashort light pulses, large-bandwidth FEL, ultrahigh peak power, and polarization control and compact FEL facilities. In order to realize the full promise of FEL, one of the primary goals for future development is the generation of fully coherent FELs, which has attracted great attention since the first light of SASE X-rays at the LCLS. The generation of fully coherent FEL pulses at short wavelengths can be achieved by improving the longitudinal coherence of SASE, seeded FELs, and XFELs. All of these potential methods have their advantages and disadvantages and are now being investigated vigorously.

Along with rapid construction and commissioning of FELs worldwide, the development of FELs in China is highly successful. After decades of vigorous development beginning in the 1980s, FEL facilities in China now include low-gain FELs and high-gain FELs covering wavelengths from terahertz to hard X-rays. One of the most fruitful FEL facilities is the SDUV-FEL, where successful realization of SASE, HGHG, and EEHG has paved the way for construction of user facilities, including the DCLS, SXFEL, and SHINE. Even more promising is that construction recently began on the first hard X-ray FEL facility in China, SHINE, which employs an advanced

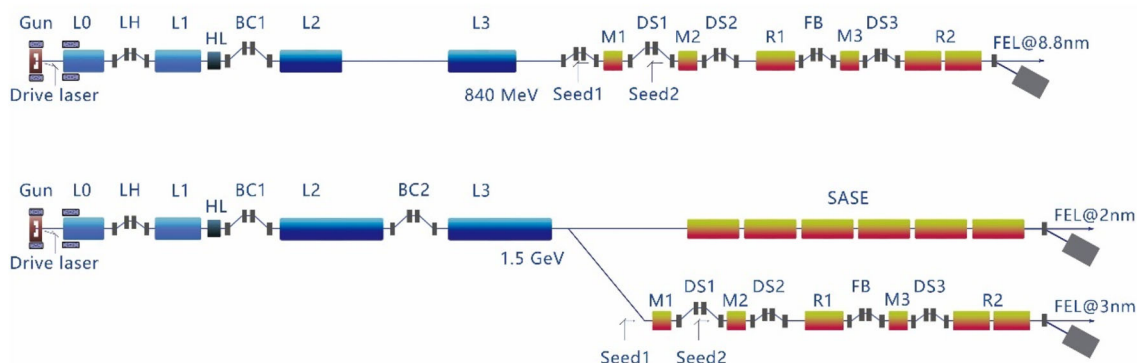


Fig. 10 (Color online) Schematic layouts: SXFEL-TF (top) and SXFEL-UF (bottom) (LH—laser heater, HL—harmonic linearizer, BC—bunch compressor, M—modulator, DS—dispersion section, R—radiator, FB—fresh bunch)

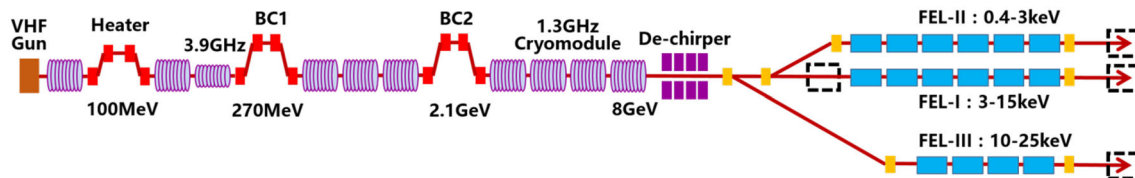


Fig. 11 (Color online) Layout of the SHINE project

superconducting accelerator and FEL schemes to provide a high-repetition-rate, high-brightness, fully coherent X-ray FEL.

Acknowledgements The authors would like to thank Li Zeng, Kai Li, Bo Liu, Dong Wang, and Zhen-Tang Zhao from SINAP; Wei-Qing Zhang from DICP; Dai Wu from CAEP; Yi Jiao from IHEP; and He-Ting Li from USTC for helpful suggestions and useful comments.

References

- P. Emma, R. Akre, J. Arthur et al., First lasing and operation of an angstrom-wavelength free-electron laser. *Nat. Photonics* **4**, 641–647 (2010). <https://doi.org/10.1038/nphoton.2010.176>
- T. Ishikawa, H. Aoyagi, T. Asaka et al., A compact X-ray free-electron laser emitting in the sub-angstrom region. *Nat. Photonics* **6**, 540 (2012). <https://doi.org/10.1038/nphoton.2012.141>
- H.S. Kang, C.K. Min, H. Heo et al., Hard X-ray free-electron laser with femtosecond-scale timing jitter. *Nat. Photonics* **11**, 708 (2017). <https://doi.org/10.1038/s41566-017-0029-8>
- C. Milne, T. Schietinger, M. Aiba, SwissFEL: the Swiss X-ray free electron laser. *Appl. Sci.* **7**, 720 (2017). <https://doi.org/10.3390/app7070720>
- M. Altarelli, R. Brinkmann, M. Chergui et al., *The European X-Ray Free-electron Laser*, Technical Design Report, DESY (2007)
- J. N. Galayda, The linac coherent light source-II project, in *Proceedings of IPAC'14*, Dresden, Germany, p. 935 (2014)
- Z. Zhu, Z. Zhao, D. Wang, et al., SCLF: An 8-GeV CW SCRF linac-based X-ray FEL facility in Shanghai, in *Proceedings of FEL2017*, Santa Fe, NM, USA, p. 182 (2017). <https://doi.org/10.18429/JACoW-FEL2017-MOP055>
- E.L. Saldin, E.A. Schneidmiller, M.V. Yurkov, Terawatt-scale sub-10-fs laser technology- key to generation of GW-level attosecond pulses in X-ray free electron laser. *Opt. Commun.* **237**, 153 (2004). <https://doi.org/10.1016/j.optcom.2004.03.070>
- A.A. Zholents, M.S. Zolotorev, Attosecond x-ray pulses produced by ultra short transverse slicing via laser electron beam interaction. *New J. Phys.* **10**, 025005 (2008). <https://doi.org/10.1088/1367-2630/10/2/025005>
- J. Qiang, J. Wu, Generation of multi-color attosecond X-ray radiation through modulation compression. *Appl. Phys. Lett.* **99**, 081101 (2011). <https://doi.org/10.1063/1.3629769>
- E. Prat, S. Reiche, Simple method to generate terawatt-attosecond X-ray free-electron-laser pulses. *Phys. Rev. Lett.* **114**, 244801 (2015). <https://doi.org/10.1103/PhysRevLett.114.244801>
- J.B. Rosenzweig, D. Alesini, G. Andonian, Generation of ultra-short, high brightness electron beams for single-spike SASE FEL operation. *Nucl. Instrum. Methods A* **593**, 39 (2008). <https://doi.org/10.1016/j.nima.2008.04.083>
- S. Huang, Y. Ding, Y. Feng, Generating single-spike hard X-ray pulses with nonlinear bunch compression in free-electron lasers. *Phys. Rev. Lett.* **119**, 154801 (2017). <https://doi.org/10.1103/PhysRevLett.119.154801>
- A.S. Hernandez, E. Prat, S. Bettoni, Generation of large-bandwidth x-ray free-electron-laser pulses. *Phys. Rev. Lett.* **19**, 090702 (2016). <https://doi.org/10.1103/PhysRevAccelBeams.19.090702>
- I. Zagorodnov, G. Feng, T. Limberg, Corrugated structure insertion for extending the SASE bandwidth up to 3% at the European XFEL. *Nucl. Instrum. Methods* **837**, 69–79 (2016). <https://doi.org/10.1016/j.nima.2016.09.001>
- S. Serkez, V. Kocharyan, E. Saldin, et al., Report No. DESY 13-109. Deutsches Elektronen-Synchrotron, Hamburg, Germany (2013)
- E. Prat, M. Calvi, S. Reiche, Generation of ultra-large-bandwidth X-ray free-electron-laser pulses with a transverse-gradient undulator. *J. Synchrotron Radiat.* **23**, 874–879 (2016). <https://doi.org/10.1107/S1600577516007177>
- M. Song, J. Yan, K. Li, C. Feng et al., Bandwidth broadening of X-ray free electron laser pulses with the natural gradient of planar undulator. *Nucl. Instrum. Methods* **884**, 11–17 (2018). <https://doi.org/10.1016/j.nima.2017.12.005>
- R. Neutze, R. Wouts, D. van der Spoel et al., Potential for biomolecular imaging with femtosecond X-ray pulses. *Nature (London)* **406**, 752 (2000). <https://doi.org/10.1038/35021099>
- M. Fuchs, M. Trigo, J. Chen, Anomalous nonlinear X-ray Compton scattering. *Nat. Phys.* **11**, 964 (2015). <https://doi.org/10.1038/nphys3452>
- N.M. Kroll, P.L. Morton, M. Rosenbluth, Free-electron lasers with variable parameter wigglers. *IEEE J. Quantum Electron.* **17**, 1436 (1981). <https://doi.org/10.1109/JQE.1981.1071285>
- W.M. Fawley, Z. Huang, K.J. Kim, Tapered undulators for SASE FELs. *Nucl. Instrum. Methods A* **483**, 537–541 (2002). [https://doi.org/10.1016/S0168-9002\(02\)00377-7](https://doi.org/10.1016/S0168-9002(02)00377-7)
- W.M. Fawley, J. Frisch, Z. Huang, et al., Toward TW-level, hard X-ray pulses at LCLS, in *Proceedings of FEL2011*, Shanghai, China, pp. 160–163 (2011)
- Y. Jiao, Y. Cai, A.W. Chao et al., Modeling and multi-dimensional optimization of a tapered free electron laser. *Phys. Rev. ST Accel. Beams* **15**, 050704 (2012). <https://doi.org/10.1103/PhysRevSTAB.15.050704>
- N. Sudar, P. Musumeci, J. Duris, High efficiency energy extraction from a relativistic electron beam in a strongly tapered undulator. *Phys. Rev. Lett.* **117**, 174801 (2016). <https://doi.org/10.1103/PhysRevLett.117.174801>
- J. Faure, Y. Glinec, A. Pukhov et al., A laser-plasma accelerator producing monoenergetic electron beams. *Nature* **431**, 541–544 (2004). <https://doi.org/10.1038/nature02963>
- V.N. Litvinenko, B. Burnham, M. Emamian, Gamma-ray production in a storage ring free-electron laser. *Phys. Rev. Lett.* **78**, 4569 (1997). <https://doi.org/10.1103/PhysRevLett.78.4569>
- N.B. Aetukuri, A.X. Gray, M. Drouard et al., Control of the metal-insulator transition in vanadium dioxide by modifying orbital occupancy. *Nat. Phys.* **9**, 661 (2013). <https://doi.org/10.1038/nphys2733>
- C. von Korff Schmising, B. Pfau, M. Schneider, Imaging ultrafast demagnetization dynamics after a spatially localized

- optical excitation. *Phys. Rev. Lett* **112**, 217203 (2014). <https://doi.org/10.1103/PhysRevLett.112.217203>
30. K.J. Kim, Circular polarization with crossed-planar undulators in high-gain FELs. *Nucl. Instrum. Methods A* **445**, 329–332 (2000). [https://doi.org/10.1016/S0168-9002\(00\)00137-6](https://doi.org/10.1016/S0168-9002(00)00137-6)
 31. H. Deng, T. Zhang, L. Feng, Polarization switching demonstration using crossed-planar undulators in a seeded free-electron laser. *Phys. Rev. ST Accel. Beams* **17**, 020704 (2014). <https://doi.org/10.1103/PhysRevSTAB.17.020704>
 32. E. Ferrari, E. Allaria, J. Buck, Single shot polarization characterization of XUV FEL pulses from crossed polarized undulators. *Sci. Rep.* **5**, 13531 (2015). <https://doi.org/10.1038/srep13531>
 33. E. Allaria, B. Diviacco, C. Callegari et al., Control of the polarization of a vacuum-ultraviolet, high-gain, free-electron laser. *Phys. Rev. X* **4**, 41040 (2014). <https://doi.org/10.1103/PhysRevX.4.041040>
 34. A.A. Lutman, J.P. Macarthur, M. Ilchen et al., Polarization control in an X-ray free-electron laser. *Nat. Photonics* **10**, 468–472 (2016). <https://doi.org/10.1038/nphoton.2016.79>
 35. J.M.J. Madey, Stimulated emission of bremsstrahlung in a periodic magnetic field. *J. Appl. Phys.* **42**, 1906 (1971). <https://doi.org/10.1063/1.1660466>
 36. D. Deacon, L. Elias, J. Madey, First operation of a free-electron laser. *Phys. Rev. Lett.* **38**, 892 (1977). <https://doi.org/10.1103/PhysRevLett.38.892>
 37. D. Oepts, A.F.G. Van der Meer, P.W. Van Amersfoort, The free-electron-laser user facility FELIX. *Infrared Phys. Techn.* **36**, 297–308 (1995). [https://doi.org/10.1016/1350-4495\(94\)00074-U](https://doi.org/10.1016/1350-4495(94)00074-U)
 38. A.M. Kondratenko, E.L. Saldin, Generating of coherent radiation by a relativistic electron beam in an undulator. *Part. Accel.* **10**, 207–216 (1980)
 39. R. Bonifacio, C. Pellegrini, L.M. Narducci, Collective instabilities and high-gain regime in a free electron laser. *Opt. Commun.* **50**, 373–378 (1984). [https://doi.org/10.1016/0030-4018\(84\)90105-6](https://doi.org/10.1016/0030-4018(84)90105-6)
 40. B.D. Patterson, R. Abela, Novel opportunities for time-resolved absorption spectroscopy at the X-ray free electron laser. *Phys. Chem. Chem. Phys.* **12**, 5647–5652 (2010). <https://doi.org/10.1039/C003406A>
 41. J.B. Murphy, C. Pellegrini, Generation of high-intensity coherent radiation in the soft-x-ray and vacuum-ultraviolet region. *J. Opt. Soc. Am. B* **2**, 259 (1985). <https://doi.org/10.1364/JOSAB.2.000259>
 42. M.J. Hogan, C. Pellegrini, J. Rosenzweig, Measurements of high gain and intensity fluctuations in a self-amplified, spontaneous-emission free-electron laser. *Phys. Rev. Lett.* **80**, 289 (1998). <https://doi.org/10.1103/PhysRevLett.80.289>
 43. W. Ackermann, G. Asova, V. Ayvazyan et al., Operation of a free-electron laser from the extreme ultraviolet to the water window. *Nat. Photonics* **1**, 336–342 (2007). <https://doi.org/10.1038/nphoton.2007.76>
 44. C. Bostedt, S. Boutet, D.M. Fritz, Linac coherent light source: the first five years. *Rev. Mod. Phys.* **88**, 015007 (2016). <https://doi.org/10.1103/RevModPhys.88.015007>
 45. J. Feldhaus, E.L. Saldin, Possible application of X-ray optical elements for reducing the spectral bandwidth of an X-ray SASE FEL. *Opt. Commun.* **140**, 341 (1997). [https://doi.org/10.1016/S0030-4018\(97\)00163-6](https://doi.org/10.1016/S0030-4018(97)00163-6)
 46. G. Geloni, V. Kocharyan, E. Saldin, A novel self-seeding scheme for hard X-ray FELs. *J. Mod. Opt.* **58**, 1391 (2011). <https://doi.org/10.1080/09500340.2011.586473>
 47. C. Feng, *Theoretical and Experimental Studies on Novel High-Gain Seeded Free-Electron Laser Schemes* (Springer, Berlin, 2016)
 48. D. Ratner, R. Abela, J. Amann, Experimental demonstration of a soft X-ray self-seeded free-electron laser. *Phys. Rev. Lett.* **114**, 054801 (2015). <https://doi.org/10.1103/PhysRevLett.114.054801>
 49. J. Amann, W. Berg, V. Blank et al., Demonstration of self-seeding in a hard-X-ray free-electron laser. *Nat. Photonics* **6**, 693 (2012). <https://doi.org/10.1038/nphoton.2012.180>
 50. K. Zhang, Z. Qi, C. Feng, Extending the photon energy coverage of an x-ray self-seeding FEL via the reverse taper enhanced harmonic generation technique. *Nucl. Instrum. Methods A* **854**, 3–10 (2017). <https://doi.org/10.1016/j.nima.2017.02.039>
 51. K. Zhang, L. Zeng, Z. Qi, Eliminating the microbunching-instability-induced sideband in a soft X-ray self-seeding free-electron laser. *Nucl. Instrum. Methods A* **882**, 22–29 (2017). <https://doi.org/10.1016/j.nima.2017.10.060>
 52. H. Zhang, K. Li, J. Yan, Atomic inner-shell radiation seeded free-electron lasers. *Phys. Rev. ST Accel. Beams* **21**, 070701 (2018). <https://doi.org/10.1103/PhysRevAccelBeams.21.070701>
 53. B.W.J. McNeil, N.R. Thompson, D.J. Dunning, Transform-limited X-ray pulse generation from a high-brightness self-amplified spontaneous-emission free-electron laser. *Phys. Rev. Lett.* **110**, 134802 (2013). <https://doi.org/10.1103/PhysRevLett.110.134802>
 54. J. Wu, F.-J. Decker, Y. Feng, et al. X-ray Spectra and Peak Power Control with iSASE, in *Proceedings of IPAC13* (Shanghai, China), p. 2068 (2013)
 55. D. Xiang, Y. Ding, Z. Huang et al., Purified self-amplified spontaneous emission free-electron lasers with slippage-boosted filtering. *Phys. Rev. ST Accel. Beams* **16**, 010703 (2013). <https://doi.org/10.1103/PhysRevSTAB.16.010703>
 56. E.A. Schneidmiller, M.V. Yurkov, Harmonic lasing in X-ray free electron lasers. *Phys. Rev. ST Accel. Beams* **15**, 080702 (2012). <https://doi.org/10.1103/PhysRevSTAB.15.080702>
 57. E.A. Schneidmiller, B. Faatz, M. Kuhlmann, First operation of a harmonic lasing self-seeded free electron laser. *Phys. Rev. ST Accel. Beams* **20**, 020705 (2017). <https://doi.org/10.1103/PhysRevAccelBeams.20.020705>
 58. G. Lambert, T. Hara, D. Garzella et al., Injection of harmonics generated in gas in a free-electron laser providing intense and coherent extreme-ultraviolet light. *Nat. Phys.* **4**, 296 (2008). <https://doi.org/10.1038/nphys889>
 59. T. Togashi, K. Fukami, S. Matsubara, et al., First Observation of the 61.5 nm Seeded FEL at the SCSS Test Accelerator, in *Proceedings of the 2010 FEL Conference*, Malmö, Sweden (2010)
 60. S. Ackermann, A. Azima, J. Bödewadt, et al., sFLASH - Present Status and Commissioning Results, in *Proceedings of IPAC2011*, San Sebastián, Spain, pp. 923–927 (2011)
 61. L.H. Yu, Generation of intense uv radiation by subharmonically seeded single-pass free-electron lasers. *Phys. Rev. A* **44**, 5178 (1991). <https://doi.org/10.1103/PhysRevA.44.5178>
 62. L.H. Yu, M. Babzien, I. Ben-Zvil et al., High-gain harmonic-generation free-electron laser. *Science* **289**, 932 (2000). <https://doi.org/10.1126/science.289.5481.932>
 63. L.-H. Yu, I. Ben-Zvi, High-gain harmonic generation of soft X-rays with the “fresh bunch” technique. *Nucl. Instrum. Methods A* **393**, 96–99 (1997). [https://doi.org/10.1016/S0168-9002\(97\)00435-X](https://doi.org/10.1016/S0168-9002(97)00435-X)
 64. J. Wu, L.H. Yu, Coherent hard X-ray production by cascading stages of high gain harmonic generation. *Nucl. Instrum. Methods A* **475**, 104–111 (2001). [https://doi.org/10.1016/S0168-9002\(01\)01552-2](https://doi.org/10.1016/S0168-9002(01)01552-2)
 65. E. Allaria, D. Castronovo, P. Cinquegrana et al., Two-stage seeded soft-X-ray free-electron laser. *Nat. Photonics* **7**, 913–918 (2013). <https://doi.org/10.1038/nphoton.2013.277>

66. Z. Zhao, D. Wang, Q. Gu, SXFEL: a soft X-ray free electron laser in China. *Synchrotron Radiat News* **30**, 29–33 (2017). <https://doi.org/10.1080/08940886.2017.1386997>
67. G. Stupakov, Using the beam-echo effect for generation of short-wavelength radiation. *Phys. Rev. Lett.* **102**, 074801 (2009). <https://doi.org/10.1103/PhysRevLett.102.074801>
68. D. Xiang, G. Stupakov, Echo-enabled harmonic generation free electron laser. *Phys. Rev. ST Accel. Beams* **12**, 030702 (2009). <https://doi.org/10.1103/PhysRevSTAB.12.030702>
69. D. Xiang, E. Colby, M. Dunning, Demonstration of the echo-enabled harmonic generation technique for short-wavelength seeded free electron lasers. *Phys. Rev. Lett.* **105**, 114801 (2010). <https://doi.org/10.1103/PhysRevLett.105.114801>
70. D. Xiang, E. Colby, M. Dunning, Evidence of high harmonics from echo-enabled harmonic generation for seeding X-ray free electron lasers. *Phys. Rev. Lett.* **108**, 024802 (2012). <https://doi.org/10.1103/PhysRevLett.108.024802>
71. Z. Zhao, D. Wang, J. Chen et al., First lasing of an echo-enabled harmonic generation free-electron laser. *Nat. Photonics* **6**, 360–363 (2012). <https://doi.org/10.1038/nphoton.2012.105>
72. E. Hemsing, M. Dunning, B. Garcia et al., Echo-enabled harmonics up to the 75th order from precisely tailored electron beams. *Nat. Photonics* **10**, 512–515 (2016). <https://doi.org/10.1038/nphoton.2016.101>
73. C. Feng, D. Huang, H. Deng et al., A single stage EEHG at SXFEL for narrow-bandwidth soft X-ray generation. *Sci. Bull.* **61**, 1202 (2016). <https://doi.org/10.1007/s11434-016-1060-8>
74. C. Feng, Z.T. Zhao, Hard X-ray free-electron laser based on echo-enabled staged harmonic generation scheme. *Chin. Sci. Bull.* **55**, 221–227 (2010). <https://doi.org/10.1007/s11434-010-0002-0>
75. Z. Zhao, C. Feng, J. Chen et al., Two-beam based two-stage EEHG-FEL for coherent hard X-ray generation. *Sci. Bull.* **61**, 720–727 (2016). <https://doi.org/10.1007/s11434-016-1060-8>
76. Z. Zhao, C. Feng, K.Q. Zhang, Two-stage EEHG for coherent hard X-ray generation based on a superconducting linac. *Nucl. Sci. Tech.* **28**, 117 (2017). <https://doi.org/10.1007/s41365-017-0258-z>
77. H. Deng, C. Feng, Using off-resonance laser modulation for beam-energy-spread cooling in generation of short-wavelength radiation. *Phys. Rev. Lett.* **111**, 084801 (2013). <https://doi.org/10.1103/PhysRevLett.111.084801>
78. C. Feng, H. Deng, D. Wang, Phase-merging enhanced harmonic generation free-electron laser. *New J. Phys.* **16**, 043021 (2014). <https://doi.org/10.1088/1367-2630/16/4/043021>
79. C. Feng, T. Zhang, H. Deng, Three-dimensional manipulation of electron beam phase space for seeding soft X-ray free-electron lasers. *Phys. Rev. ST Accel. Beams* **17**, 070701 (2014). <https://doi.org/10.1103/PhysRevSTAB.17.070701>
80. W. Liu, Y. Jiao, *IPAC 2018, TUPMF051* (Vancouver, BC, Canada, 2018)
81. Q. Jia, H. Li, Normal planar undulators doubling as transverse gradient undulators. *Phys. Rev. ST Accel. Beams* **20**, 020707 (2017). <https://doi.org/10.1103/PhysRevAccelBeams.20.020707>
82. Z. Zhao, H. Li, Q. Jia, Phase-merging enhanced harmonic generation free-electron laser with a normal modulator. *J. Synchrotron Radiat.* **24**, 906–911 (2017). <https://doi.org/10.1107/S1600577517008402>
83. Z. Qi, C. Feng, H. Deng, Parameter optimization and start-to-end simulation for the phase-merging enhanced harmonic generation free electron laser. *Nucl. Instrum. Methods A* **875**, 119–124 (2017). <https://doi.org/10.1016/j.nima.2017.08.059>
84. Y.V. Shvyd'ko, S. Stoupin, A. Cunsolo et al., High-reflectivity high-resolution X-ray crystal optics with diamonds. *Nat. Phys.* **6**, 196 (2010). <https://doi.org/10.1038/nphys1506>
85. K.J. Kim, Y.V. Shvyd'ko, S. Reiche, A proposal for an X-ray free-electron laser oscillator with an energy-recovery linac. *Phys. Rev. Lett.* **100**, 244802 (2008). <https://doi.org/10.1103/PhysRevLett.100.244802>
86. K. J. Kim, T. Maxwell, R. Lindberg, et al., An oscillator configuration for full realization of hard X-ray free electron laser, in *Proceedings of IPAC2016*, Busan, Korea, pp. 801–804 (2016). <https://doi.org/10.18429/JACoW-IPAC2016-MOPOW039>
87. Y.V. Shvyd'ko, R. Lindberg, Spatiotemporal response of crystals in X-ray Bragg diffraction. *Phys. Rev. ST Accel. Beams* **15**, 100702 (2012). <https://doi.org/10.1103/PhysRevSTAB.15.100702>
88. K.J. Kim, Y.V. Shvyd'ko, Tunable optical cavity for an X-ray free-electron-laser oscillator. *Phys. Rev. ST Accel. Beams* **12**, 030703 (2009). <https://doi.org/10.1103/PhysRevSTAB.12.030703>
89. K. Li, H. Deng, Systematic design and three-dimensional simulation of X-ray FEL oscillator for Shanghai coherent light facility. *Nucl. Instrum. Methods A* **895**, 40 (2018). <https://doi.org/10.1016/j.nima.2018.03.072>
90. K. Li, M. Song, H. Deng, Simplified model for fast optimization of a free-electron laser oscillator. *Phys. Rev. ST Accel. Beams* **20**, 030702 (2017). <https://doi.org/10.1103/PhysRevAccelBeams.20.030702>
91. K. Li, H. Deng, Gain cascading scheme of a free-electron-laser oscillator. *Phys. Rev. ST Accel. Beams* **20**, 110703 (2017). <https://doi.org/10.1103/PhysRevAccelBeams.20.110703>
92. K. Li, J. Yan, C. Feng, High brightness fully coherent X-ray amplifier seeded by a free-electron laser oscillator. *Phys. Rev. ST Accel. Beams* **21**, 040702 (2018). <https://doi.org/10.1103/PhysRevAccelBeams.21.040702>
93. J. Dai, H. Deng, Z. Dai, Proposal for an X-ray free electron laser oscillator with intermediate energy electron beam. *Phys. Rev. Lett.* **108**, 034802 (2012). <https://doi.org/10.1103/PhysRevLett.108.034802>
94. B.W. Adams, K.J. Kim, X-ray comb generation from nuclear-resonance-stabilized X-ray free-electron laser oscillator for fundamental physics and precision metrology. *Phys. Rev. ST Accel. Beams* **18**, 030711 (2015). <https://doi.org/10.1103/PhysRevSTAB.18.030711>
95. K. Li, H. Deng, Gain-guided X-ray free-electron laser oscillator. *Appl. Phys. Lett.* **113**, 061106 (2018). <https://doi.org/10.1063/1.5037180>
96. T. Kolodziej, Y. Shvyd'ko, D. Shu, Efficiency and coherence preservation studies of Be refractive lenses for XFEL application. *J. Synchrotron Radiat.* **25**, 354–360 (2018). <https://doi.org/10.1107/S160057751701699X>
97. J. Xie, J. Zhuang, Y. Huang, First lasing of the Beijing FEL. *Nucl. Instrum. Methods A* **341**, p34–38 (1994). [https://doi.org/10.1016/0168-9002\(94\)90312-3](https://doi.org/10.1016/0168-9002(94)90312-3)
98. M. Li, X. Jin, Z. Xu, First Lasing of the CAEP FIR-FEL, in *Proceeding of FEL2005*, Palo Alto, CA, USA, pp. e-proc. MOOB005 (2005)
99. X. Jin, M. Li, Z. Xu, Experiment study on the CAEP FIR-FEL. *Chin. Phys. C* **30**, 96–98 (2006)
100. Z. Xu, X. Yang, M. Li, Design of a high average power terahertz-FEL facility. *J. Terahertz Sci. Electron. Inf. Technol.* **11**, p1–6 (2013)
101. M. Li, X. Yang, Z. Xu, et al., First lasing of CAEP THz free electron laser. *High Power Laser Part. Beam.* **29**(10), p1–2 (2017). <https://doi.org/10.11884/HPLPB201729.170363>
102. M. Li, X. Yang, Z. Xu et al., Experimental study on the stimulated saturation of terahertz free electron laser. *Acta Phys. Sin.* **67**(8), 084102 (2018). <https://doi.org/10.7498/aps.67.20172413>
103. H. Li, Q. Jia, S. Zhang et al., Design of FELiChEM, the first infrared free-electron laser user facility in China. *Chin. Phys. C*

- 41(1), 018102 (2017). <https://doi.org/10.1088/1674-1137/41/1/018102>
104. H. Li, Z. He, Q. Jia, et al., Status of FELiCHEM, a new IR-FEL in China, in *Proceedings of IPAC2016*, Busan, Korea, pp. P774–776 (2016). <https://doi.org/10.18429/JACoW-IPAC2016-MOPOW026>
105. Z. Zhao, H. Li, Q. Jia, Effect of cavity length detuning on the output characteristics for the middle infrared FEL oscillator of FELiChEM. *Chin. Phys. C* **41**(10), 108101 (2017). <https://doi.org/10.1088/1674-1137/41/10/108101>
106. Z. Zhao, The Shanghai high-gain harmonic generation DUV free-electron laser. *Nucl. Instrum. Methods A* **393**, 96–99 (2004). <https://doi.org/10.1016/j.nima.2004.04.108>
107. Z. Zhao, D. Wang, Seeded FEL experiments at the SDUV–FEL test facility. *IEEE T. Nucl. Sci.* **63**, 930–938 (2016). <https://doi.org/10.1016/B978-0-444-51727-2.50129-2>
108. C. Feng, T. Zhang, J. Chen et al., Measurement of the average local energy spread of electron beam via coherent harmonic generation. *Phys. Rev. ST Accel. Beams* **14**, 090701 (2011). <https://doi.org/10.1103/PhysRevSTAB.14.090701>
109. H. Deng, M. Zhang, C. Feng, Experimental demonstration of longitudinal beam phase-space linearizer in a free-electron laser facility by corrugated structures. *Phys. Rev. Lett.* **113**, 254802 (2014). <https://doi.org/10.1103/PhysRevLett.113.254802>
110. B. Liu, W.B. Li, J.H. Chen et al., Demonstration of a widely-tunable and fully-coherent high-gain harmonic-generation free-electron laser. *Phys. Rev. ST Accel. Beams* **16**, 020704 (2013). <https://doi.org/10.1103/PhysRevSTAB.16.020704>
111. H. Wang, Y. Yu, Y. Chang et al., Photodissociation dynamics of H₂O at 111.5 nm by a vacuum ultraviolet free electron laser. *J. Chem. Phys.* **148**, 124301 (2018). <https://doi.org/10.1063/1.5022108>
112. Z. Zhao, D. Wang, Q. Gu, Status of the SXFEL facility. *Appl. Sci.* **7**, 607 (2017). <https://doi.org/10.3390/app7060607>
113. Z. Zhao, D. Wang, Q. Gu, SXFEL: a soft X-ray free electron laser in China. *Synchrotron Radiat. News* **30**, 29 (2017). <https://doi.org/10.1080/08940886.2017.1386997>